General parameterization of Auger recombination in crystalline silicon

Mark J. Kerr[a] and Andres Cuevas
Centre for Sustainable Energy Systems, Department of Engineering, Australian National University, Canberra ACT 0200, Australia

(Received 6 August 2001; accepted for publication 12 November 2001)

A parameterization for band-to-band Auger recombination in silicon at 300 K is proposed. This general parameterization accurately fits the available experimental lifetime data for arbitrary injection level and arbitrary dopant density, for both *n*-type and *p*-type dopants. We confirm that Auger recombination is enhanced above the traditional free-particle rate at both low injection and high injection conditions. Further, the rate of enhancement is shown to be less for highly injected intrinsic silicon than for lowly injected doped silicon, consistent with the theory of Coulomb-enhanced Auger recombination. Variations on the parameterization are discussed. [DOI: 10.1063/1.1432476]

I. INTRODUCTION

Auger recombination can significantly influence the performance of many silicon devices. The base region of power transistors[1] and high efficiency photovoltaic cells[2] are affected by it under high injection conditions, while the quantum efficiency and saturation current of heavily doped emitters[3] can be affected at low injection conditions. Accurate models for determining the rate of Auger recombination as a function of injection level and doping density are therefore essential, particularly for device simulation.

Traditionally, Auger recombination is viewed as a three-particle interaction where a conduction band electron and a valence band hole recombine, with the excess energy being transferred to a third free electron or hole.[4] The charge carriers involved are assumed to be noninteracting quasifree particles.[5] The *eeh* process denotes when the excess energy is transferred to another electron, with the recombination rate given by $R_{eeh}=C_n n^2 p$. Similarly, the *ehh* process denotes when the excess energy is transferred to another hole, with recombination rate $R_{ehh}=C_p n p^2$, where n and p are the free electron and hole concentrations and C_n and C_p the Auger coefficients. The total Auger recombination rate, R, is then given by

$$R_{\text{Auger}}=C_n n^2 p + C_p n p^2, \tag{1}$$

from which the common relationships for the Auger lifetime in *n*-type and *p*-type material under low injection (τ_{li}) and high injection conditions (τ_{hi}) can be determined. For *n*-type

$$\tau_{\text{li}}=\frac{1}{C_n N_D^2} \quad \text{and} \quad \tau_{\text{hi}}=\frac{1}{(C_n+C_p)\Delta p^2}, \tag{2}$$

and for *p*-type

$$\tau_{\text{li}}=\frac{1}{C_p N_A^2} \quad \text{and} \quad \tau_{\text{hi}}=\frac{1}{(C_n+C_p)\Delta n^2}, \tag{3}$$

where N_D and N_A are the density of donor and acceptor atoms, Δn and Δp are the excess carrier densities, and $C_a \equiv C_n+C_p$ is the ambipolar Auger coefficient. From Eqs. (2) and (3), it can be seen that the Auger lifetime *ideally* depends on the inverse of the carrier density squared ($\tau_A \propto 1/n^2$). The most commonly quoted values for the Auger coefficients appear to be those determined by Dziewior and Schmid ($C_n = 2.8\times10^{-31}$ cm^6 s^{-1} and $C_p = 0.99\times10^{-31}$ cm^6 s^{-1}) for silicon with a doping concentration greater than 5×10^{18} cm^{-3}.[6] The implied value for the ambipolar Auger coefficient is then $C_a = 3.79\times10^{-31}$ cm^6 s^{-1}.

In reality, however, Auger recombination is more complicated. Band-to-band Auger processes can occur with phonon participation [phonon-assisted Auger recombination (PAAR)] and without phonon participation [direct Auger recombination (DAR)] to conserve momentum. PAAR is believed to dominate in *p*-type silicon while DAR is the dominant process in *n*-type silicon.[7] For nondegenerate material, both PAAR and DAR give the same dependency for the recombination rate with doping, although they are predicted to differ in degenerately doped material.[8] Further, a third Auger recombination mechanism, termed trap-assisted Auger recombination (TAAR) has been proposed by Landsberg,[9] where the lifetime depends only on the inverse of the carrier density ($\tau_{\text{TAAR}} \propto 1/n$).

The assumption that the recombining electrons and holes are noninteracting, quasifree particles has been addressed theoretically by Hangleiter and Häcker.[4] They took into account the Coulombic interaction between the mobile charge carriers and found that electrons and holes can become correlated due to the formation of excitons. The *eeh* Auger recombination rate is then strongly enhanced due to the increased electron density in the vicinity of a hole, with a similar enhancement mechanism for the *ehh* process. The strength of the Coulomb-enhancement is believed to decrease as the concentration of majority carriers increases, due to screening of the electron-hole interaction. Coulomb enhancement of Auger recombination processes therefore introduces a further departure from the ideal relationship between the Auger lifetime and doping density. This is accounted for by multiplying C_n and C_p by the enhancement factors g_{eeh} and g_{ehh}, such that

[a]Electronic mail: mark.kerr@faceng.anu.edu.au

$$\text{for } n\text{-type} \quad \tau_{\text{li}} = \frac{1}{g_{eeh} C_n N_D^2} = \frac{1}{C_n^* N_D^2}, \tag{4}$$

$$\text{and for } p\text{-type} \quad \tau_{\text{li}} = \frac{1}{g_{ehh} C_p N_A^2} = \frac{1}{C_p^* N_A^2}. \tag{5}$$

Finally, additional processes that have not yet been accounted for may impact the Auger lifetime. One such possibility is the Coulombic interactions between mobile charged carriers and fixed charges (ionized dopant atoms), which are known to be important in modeling mobilities, but do not seem to have been considered in the context of Auger recombination. It is therefore difficult to conclude what the doping and the injection level dependencies of the Auger lifetime should be from a theoretical perspective. The $1/n^2$ dependence appears to provide an upper limit on the lifetime, with the various other factors decreasing the lifetime, to a greater or lesser extent. In this article, we follow the alternative route of examining the available experimental data, including our own measurements. We then propose a formulation for the Auger recombination rate in silicon and develop a parameterization that is consistent with the observed injection level dependent lifetime data for *n*-type and *p*-type silicon of various resistivities under high and low injection conditions.

II. EXISTING ANALYTICAL MODELS

Various analytical expressions exist for estimating the Auger lifetime. Most of the models determine either the low injection Auger lifetime as a function of dopant density or the ambipolar Auger lifetime for lightly doped silicon under high injection, but not both.

A. Low injection models

The most comprehensive determination of the low injection Auger lifetime from experimental data appears to be that of Altermatt *et al.*[10] Using the C_n and C_p values of Dziewior and Schmid,[6] they performed an empirical parameterization and showed that the enhancement factors g_{eeh} and g_{ehh}, are a function of the dopant density in lowly injected silicon

$$g_{eeh}(N_D) = 1 + 44\left\{1 - \tanh\left[\left(\frac{N_D}{5\times10^{16}\ \text{cm}^{-3}}\right)^{0.34}\right]\right\}, \tag{6}$$

$$g_{ehh}(N_A) = 1 + 44\left\{1 - \tanh\left[\left(\frac{N_A}{5\times10^{16}\ \text{cm}^{-3}}\right)^{0.29}\right]\right\}. \tag{7}$$

Other authors have fit the minority carrier lifetime data for lowly injected, highly doped silicon ($N_{\text{dop}} > 1\times10^{17}\ \text{cm}^{-3}$) using an inverse quadratic expression for both *n*-type[11] and *p*-type silicon.[12] Nevertheless, Swirhun[13] noted that for *n*-type material, a better fit to the low injection Auger lifetime was

$$\tau_{\text{li}} = \frac{1}{1.9\times10^{-24} N_D^{1.65}}. \tag{8}$$

A similarly simple fit was not proposed for *p*-type material.

B. High injection models

The ambipolar Auger coefficient, C_a, has been determined by a number of authors using a variety of techniques.[14] Typical values quoted for C_a range from $1\times10^{-30}\ \text{cm}^6\ \text{s}^{-1}$ to $2\times10^{-30}\ \text{cm}^6\ \text{s}^{-1}$.[15] It has generally been found that C_a is larger than the sum of the low injection coefficients, $C_n + C_p$, determined for highly doped silicon. The discrepancy is generally explained by Coulomb enhancement,[4] whereby excitons in the highly injected silicon enhance the Auger recombination rate in the way described in Sec. I. This is supported by the recent analysis of Altermatt *et al.*[16] which determined that C_a decreases from $2.8\times10^{-30}\ \text{cm}^6\ \text{s}^{-1}$ to $1.9\times10^{-30}\ \text{cm}^6\ \text{s}^{-1}$ as the injection level in a specially designed concentrator cell (lightly doped silicon base) increased from $3\times10^{15}\ \text{cm}^{-3}$ to $1\times10^{17}\ \text{cm}^{-3}$. That is, C_a and therefore the Coulomb enhancement, is a function of the injection level.

What is not clear is if the rate of the Coulomb enhancement is the same for lowly injected, intermediate doped silicon (say $N_A = 10^{17}\ \text{cm}^{-3}$) as for highly injected, lowly doped silicon. The theory of Hangletier and Hacker predicts that the Coulomb enhancement is weaker in highly injected, lowly doped silicon. This is due to the ratio of free electrons to holes being approximately equal and so there is stronger screening of the Coulombic forces. In lowly injected, intermediate doped silicon, the concentrations of both carriers are very different, and Coulombic forces exert their full strength.

C. Complete models

There are very few models that estimate the Auger lifetime as a function of both injection level and dopant density. Experimental evidence for Coulomb-enhanced Auger recombination has been found in both lowly-injected[10] and highly-injected silicon.[16] Schmidt *et al.*[17] and Altermatt *et al.*[15] have proposed a parameterization that follows both dependencies based on the enhancement factors given in Eqs. (6) and (7). They assumed that the enhancement factors g_{eeh} and g_{ehh} depend mainly on the screening behavior of the charge carriers, and that the screening can be described by the Debye theory. This allowed them to replace the dopant density in Eqs. (6) and (7) with $n+p$. While this model has been shown to be in good agreement with experimental lifetime data for intermediately doped *p*-type silicon, it has not been tested for *n*-type silicon. Further, we will show in the following section that this model significantly overestimates the rate of Auger recombination in highly injected, lowly doped material.

A relatively simple model that changes the rate of Auger recombination in silicon as it changes from low injection to high injection conditions is used in the device simulation package PC1D.[18] This model chooses fixed values for C_n and C_p under low injection conditions (termed $C_{n,\text{li}}$ and $C_{p,\text{li}}$), and a fixed value for C_a under high injection conditions, and then weights between them to determine effective Auger coefficients, C_n^{eff} and C_p^{eff}, that can be used in Eq. (1):

$$C_n^{\text{eff}} = C_{n,\text{lli}}\left(\frac{N_D}{N_D + p}\right) + \frac{C_a}{2}\left(\frac{p}{N_D + p}\right), \tag{9}$$

$$C_p^{\text{eff}} = C_{p,\text{lli}}\left(\frac{N_A}{N_A+n}\right) + \frac{C_a}{2}\left(\frac{n}{N_A+n}\right). \tag{10}$$

As implemented in PC1D, this model tends to underestimate the rate of Auger recombination occurring in silicon, as it does not include the effects of Coulomb enhancement under low injection or high injection conditions. A variation to the model has been proposed by Glunz *et al.*[19] based on a slightly different weighting from low injection to high injection. The model of Glunz *et al.* incorporates the low level injection enhancement factors g_{eeh} and g_{ehh} of Eqs. (6) and (7) [replacing $C_{n,\text{lli}}$ at the front of Eq. (9) with $g_{eeh}C_{n,\text{lli}}$ and similarly $C_{p,\text{lli}}$ with $g_{ehh}C_{p,\text{lli}}$]; it does not, however, account for the injection level dependent Coulomb-enhancement effect under high injection. As a consequence, it underestimates the recombination rate for mid to high injection levels and overestimates it at very high injection levels, as will be shown in the following section. A further weakness of this model is that there is no physical basis for the relative weighting from low injection to high injection conditions.

III. A GENERAL AUGER PARAMETERIZATION

Any parameterization of Auger recombination in silicon must correctly model the Auger lifetime of both lowly injected silicon and highly injected silicon. Further, the parameterization must demonstrate that Auger recombination is increased above the *ideal* rate, and that the increase is a function of both the doping density and the injection level. While the theory of Coulomb enhancement can elegantly (although only qualitatively) explain the experimentally observed increase in Auger recombination from the *ideal* rate, the possibility of other physical effects cannot be discounted. Our parameterization is intended to provide the simplest functional form for the experimental observations of Auger recombination in silicon.

A. The low injection Auger lifetime

Figure 1 shows the highest low injection lifetimes experimentally measured by various authors for *n*-type silicon at 300 K. In general, the data by the various authors agree quite well, with the largest amount of scatter occurring for intermediate doping densities between 1×10^{17} cm^{-3} and 5×10^{18} cm^{-3}. A good fit to the data for $N_D>5\times10^{15}$ cm^{-3} is the simple expression

$$\tau_{\text{li}} = \frac{1}{1.8\times10^{-24}N_D^{1.65}} \quad \text{for} \quad n\text{-type silicon}, \tag{11}$$

which is consistent with the approach of Swirhun.[13] Our slightly lower coefficient of 1.8×10^{-24} is mainly due to the addition of new data points. Included in Fig. 1 are the parameterizations of Eq. (11) and that of Altermatt *et al.*[10] [from Eq. (6)]. Both parameterizations fit the data quite well with the exception of the intermediate doping densities. The fit of Altermatt *et al.* is a better match to the maximum lifetimes reported, while our fit is a better match to the average lifetime at each doping density. Comparing Eqs. (4) and (11), our fit is equivalent to determining an enhanced Auger coefficient, C_n^*, of

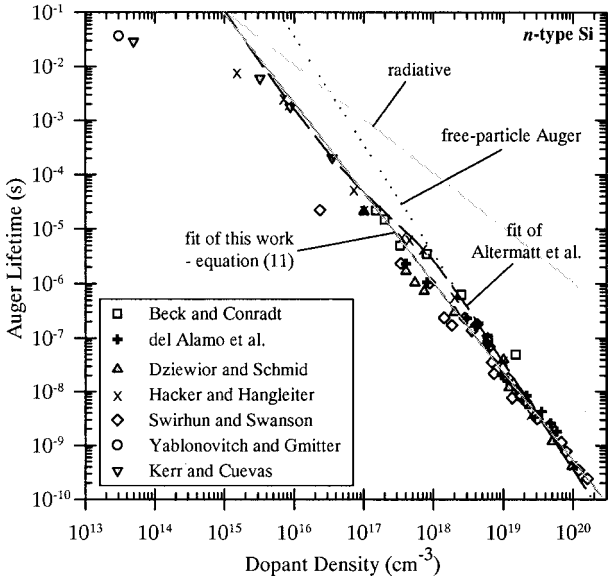

FIG. 1. Measured values of the low-injection Auger lifetime in *n*-type silicon at 300 K. The lifetime fit of this work, Eq. (11), and from Altermatt *et al.* (see Ref. 10), Eq. (6), are shown. The lifetime limit from radiative recombination and *ideal* Auger recombination are given.

$$C_n^* = g_{eeh}C_n = 1.8\times10^{-24} * N_D^{-0.35} = 1.8\times10^{-24} * n_0^{-0.35}, \tag{12}$$

which is functionally much simpler than that of Altermatt *et al.* from Eq. (6).

Similarly, Fig. 2 shows the highest low injection lifetimes experimentally measured by various authors for *p*-type silicon at 300 K. The parameterization proposed by Altermatt *et al.*[10] [from Eq. (7)] is included, along with our best fit for $N_A>5\times10^{15}$ cm^{-3}:

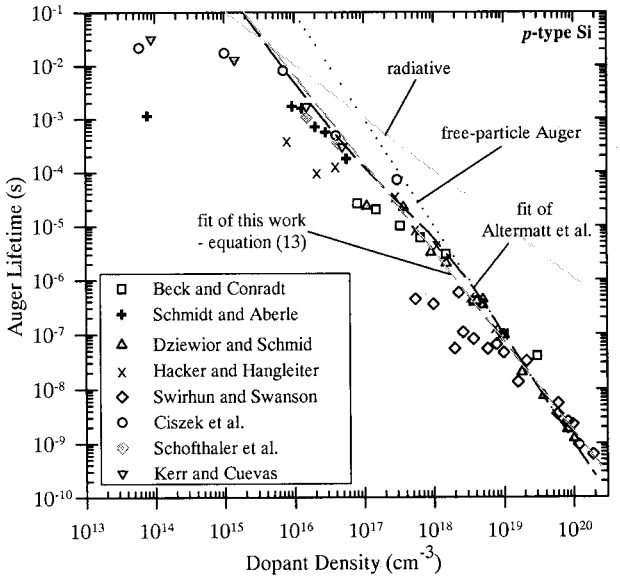

FIG. 2. Measured values of the low-injection Auger lifetime in *p*-type silicon at 300 K. The lifetime fit of this work, Eq. (13), and from Altermatt *et al.* (see Ref. 10), Eq. (7), are shown. The lifetime limit from radiative recombination and *ideal* Auger recombination are given.

$$\tau_{\rm li}=\frac{1}{6\times10^{-25}N_A^{1.65}} \quad \text{for} \quad p\text{-type silicon.} \tag{13}$$

Again, the data from the various authors agree reasonably well and both parameterizations fit within the experimental scatter. Indeed, it is difficult to conclude which parameter set is superior due to the scatter of the data, although both are quite acceptable. Comparison of Eqs. (5) and (13) show that the parameterization of Eq. (13) is equivalent to determining an enhanced Auger coefficient, C_p^*, of

$$C_p^*=g_{ehh}C_p=6\times10^{-25}*N_A^{-0.35}=6\times10^{-25}*p_0^{-0.35}. \tag{14}$$

The expressions of Eqs. (11) and (13) retain the experimental observation that the Auger recombination rate is three times stronger in heavily doped *n*-type silicon than in *p*-type silicon.

B. The high injection Auger lifetime

The highest lifetimes reported for silicon under high injection are in the vicinity of 30 ms.[20–22] The lifetime values reported by Yablonovitch *et al.*[20] are for the bulk lifetime of lightly doped *n*-type silicon. They include Auger recombination and radiative recombination. Many authors have considered the rate of radiative recombination to be negligible, but this is not the case for such high lifetimes. The radiative recombination rate is given by

$$R_{\rm rad}=Bnp, \tag{15}$$

where B is the coefficient for radiative recombination, equal to 9.5×10^{-15} cm^3 s^{-1}.[23] The high injection Auger lifetime can be found by subtracting the radiative recombination rate from the bulk lifetime data of Yablonovitch *et al.*

$$\frac{1}{\tau_{\rm Auger}}=\frac{1}{\tau_{\rm bulk}}-B(N_D+\Delta p). \tag{16}$$

Figure 3 shows the extracted Auger lifetimes. It is clear that radiative recombination is significant for injection levels from 5×10^{14} cm^{-3} to 3×10^{16} cm^{-3}. Indeed, the maximum impact of radiative recombination is at carrier densities around 2×10^{15} cm^{-3}, where the bulk lifetime was measured to be 23 ms but the Auger lifetime is determined to be 49 ms. Examination of the Auger lifetime data in Fig. 3 suggests that, even for the high lifetimes measured by Yablonovitch *et al.*, there is still evidence of a residual Shockley–Read–Hall (SRH) recombination which gives rise to the decreasing lifetime as the injection level decreases below 1×10^{15} cm^{-3}. The electron lifetime, τ_{n_0}, of this SRH center is ≈37 ms with a comparable value for the hole lifetime.

Included in Fig. 3 are our own lifetime measurements at high excess carrier densities, with radiative recombination subtracted, for 90 Ω cm *n*-type and 150 Ω cm *p*-type silicon.[22] It can be seen that for carrier densities above 1×10^{16} cm^{-3}, where Auger recombination is dominant, our measurements and that of Yablonovitch *et al.*, are in excellent agreement. Our measurements therefore confirm that such high lifetimes are reproducible and support that they represent the limit of Auger recombination in silicon under high injection conditions. They also show that there is no discernible difference between highly injected, lowly doped *n*-type and *p*-type silicon, as one would expect.

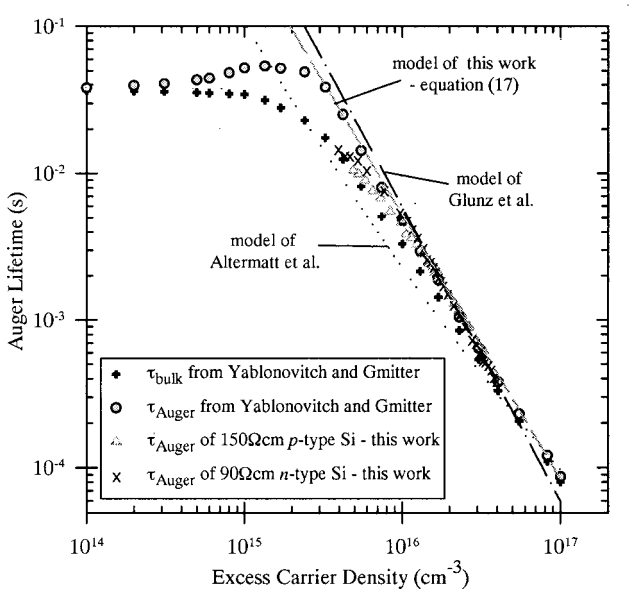

FIG. 3. The high injection bulk lifetime and Auger lifetime from Yablonovitch and Gmitter (see Ref. 20), along with our high injection Auger lifetime measurements for high resistivity *n*-type silicon (90 Ω cm) and *p*-type silicon (150 Ω cm). The predicted lifetimes from the models of Altermatt *et al.* (see Ref. 15) and Glunz *et al.* (see Ref. 19) are shown, along with the fit for the model of this work.

Also included in Fig. 3 are the predicted high injection lifetime values from the Auger model of Altermatt *et al.*,[15] as well as the modified Auger model of Glunz *et al.*[19] It can be clearly seen that the model of Altermatt *et al.* significantly overestimates Auger recombination rates in highly injected, lightly doped silicon. For example, at an injection level of 3×10^{15} cm^{-3}, the experimentally determined Auger lifetime is 38.5 ms, while the predicted Auger lifetime is only 13.9 ms. The modified Auger model of Glunz *et al.* is in better agreement with the experimental data, but it can be seen that the predicted dependence of the Auger lifetime with the injection level is incorrect. This leads to the rate of Auger recombination being overestimated for injection levels above 4×10^{16} cm^{-3}, and underestimated at lower injection levels.

A simple parameterization that, as shown in Fig. 3, properly fits the injection level dependence of the available Auger data for $\Delta p>3\times10^{15}$ cm^{-3} is

$$\tau_{\rm hi}=\frac{1}{3\times10^{-27}\Delta p^{1.8}}. \tag{17}$$

Comparison with Eq. (2) shows that this is equivalent to parameterizing an injection level dependent ambipolar Auger coefficient of

$$C_a^*=3\times10^{-27}\Delta p^{-0.2}=3\times10^{-27}\Delta n^{-0.2}. \tag{18}$$

C. A general parameterization

Experimental and theoretical considerations indicate that at least three separate parameters are required to accurately model Auger recombination. The different dominant mode

for momentum conservation during Auger recombination in *n*-type silicon (DAR) compared to *p*-type silicon (PAAR) necessitates two parameters. These parameters are not constants due to the role of Coulombic forces, which depend on the density of the mobile charges. Further, the strength of Coulombic forces is reduced depending on the ratio of free electrons to free holes, due to screening effects, and therefore a third parameter is required. We accordingly propose that Auger recombination is a three-particle process that depends on the equilibrium concentration of free electrons and free holes, and on the density of excess carriers such that the recombination rate is given by

$$R_{\text{Auger}} = np[C_1(n_0)n_0 + C_2(p_0)p_0 + C_3(\Delta n)\Delta n]. \quad (19)$$

From Eqs. (12), (14), and (18) we deduce that $C_1(n_0) = C_n^*$, $C_2(p_0) = C_p^*$ and $C_3(\Delta n) = C_a^*$, and therefore we propose a general parameterization for Auger recombination in silicon as

$$R_{\text{Auger}} = np(1.8\times10^{-24}n_0^{0.65} + 6\times10^{-25}p_0^{0.65} + 3\times10^{-27}\Delta n^{0.8}). \quad (20)$$

This parameterization accounts for the enhancement of Auger recombination due both to the dopant density and the injection level. Further, it does not assume any relative weighting of the recombination rate from low injection to high injection conditions.

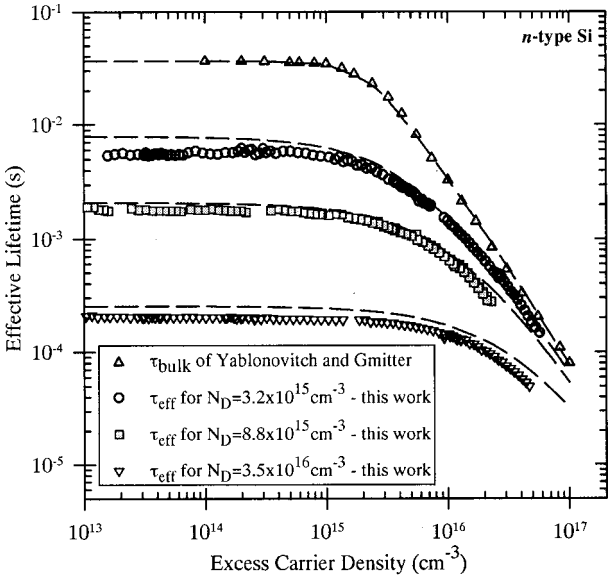

FIG. 4. Measured values for the effective lifetime as a function of excess carrier density for *n*-type silicon with doping densities up to 3.5×10^{16} cm^{-3}. The predicted values for the effective lifetime from Eq. (21) based on our parameterization of the Auger recombination rate, Eq. (20), are included. There is excellent agreement between the experimental data and the model predictions.

IV. VALIDATION OF THE AUGER PARAMETERIZATION

The proposed parameterization for Auger recombination was constructed so that it provides a good fit to the best, low injection lifetime data available in the literature as shown in Figs. 1 and 2, and also accurately fits the best high injection lifetime data. A further test of the model is to ensure that it correctly predicts the lifetime of arbitrarily doped *n*-type and *p*-type silicon from low injection through to high injection conditions. Data of this type are scarce. We have recently reported such measurements for a variety of *n*-type and *p*-type silicon wafers that were carefully passivated using *alnealed* silicon oxide.[22] Here we augment this data with measurements on silicon wafers that have been passivated with high quality plasma enhanced chemical vapor deposited silicon nitride films.[24] The combined data set constitutes a broad characterization of the effective lifetime of *n*-type and *p*-type silicon for excess carrier densities in the range of 10^{12}–10^{17} cm^{-3} and for doping densities up to 5×10^{16} cm^{-3}. These measured lifetimes are amongst the highest ever reported.

It is important to note that what has been experimentally measured is the effective lifetime, τ_{eff}, which includes all the recombination processes occurring within the silicon wafer. These processes are mainly Auger recombination (τ_{Auger}), radiative recombination (τ_{rad}), Shockley–Read–Hall recombination (τ_{SRH}), and surface recombination (τ_{surface})

$$\frac{1}{\tau_{\text{eff}}} = \frac{1}{\tau_{\text{Auger}}} + \frac{1}{\tau_{\text{rad}}} + \frac{1}{\tau_{\text{SRH}}} + \frac{1}{\tau_{\text{surface}}}. \quad (21)$$

To model the effective lifetime data we determine the Auger recombination rate from Eq. (20), the radiative recombination rate from Eq. (15) and use the SRH parameters determined from the analysis of Yablonovitch *et al.* data in Fig. 3 (i.e., $\tau_{n_0} = \tau_{p_0} = 37$ ms). This SRH contribution is only significant for samples which show effective lifetimes greater than ≈5 ms. Finally, we have not included surface recombination in the modeled lifetime, and therefore the modeled lifetime can be expected to be slightly higher than the measured lifetime, particularly for more heavily doped wafers where it is more difficult to passivate the surface.[25]

The measured effective lifetimes and predicted lifetimes are compared in Fig. 4 for *n*-type silicon. It can be seen that the predicted lifetimes fit the experimental data very well for all the doping densities and across the full range of excess carrier densities. It is important to note that radiative recombination and SRH recombination are only significant when fitting the lifetime data of Yablonovitch *et al.* Auger recombination is the prevalent recombination process in the other *n*-type samples from low injection through to high injection conditions. The proposed Auger model of Eq. (20) clearly works well for *n*-type silicon.

Figure 5 shows the measured effective lifetimes and predicted lifetimes for *p*-type silicon. Again the predicted lifetimes fit the data well for all doping densities, particularly at high injection, where Auger recombination is dominant. Again, radiative recombination and SRH bulk recombination are only significant for the high resistivity (150 Ω cm) lifetime data. It is well known that it is more difficult to passivate the surfaces of *p*-type silicon than *n*-type silicon.[25] We attribute the decreasing effective lifetime of the *p*-type samples at low injection levels to an injection level dependent surface recombination velocity. Importantly, the modeled lifetime is never lower than the measured effective life-

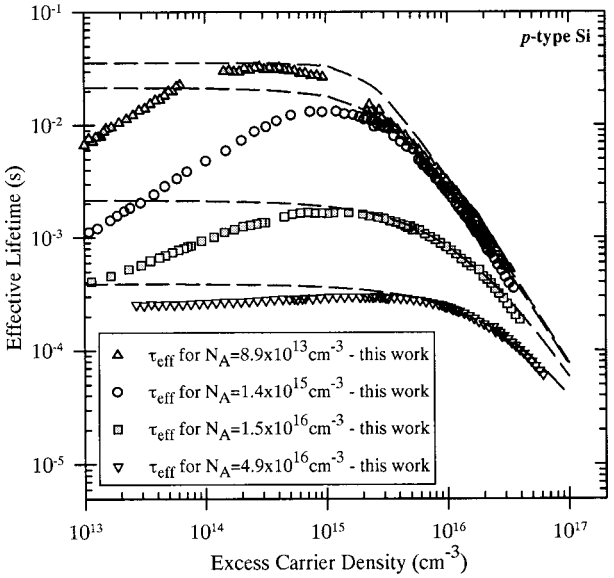

FIG. 5. Measured values for the effective lifetime as a function of excess carrier density for *p*-type silicon with doping densities up to 4.9×10^{16} cm^{-3}. The predicted values for the effective lifetime from Eq. (21) based on our parameterization of the Auger recombination rate, Eq. (20), are included. There is excellent agreement between the experimental data and the model predictions.

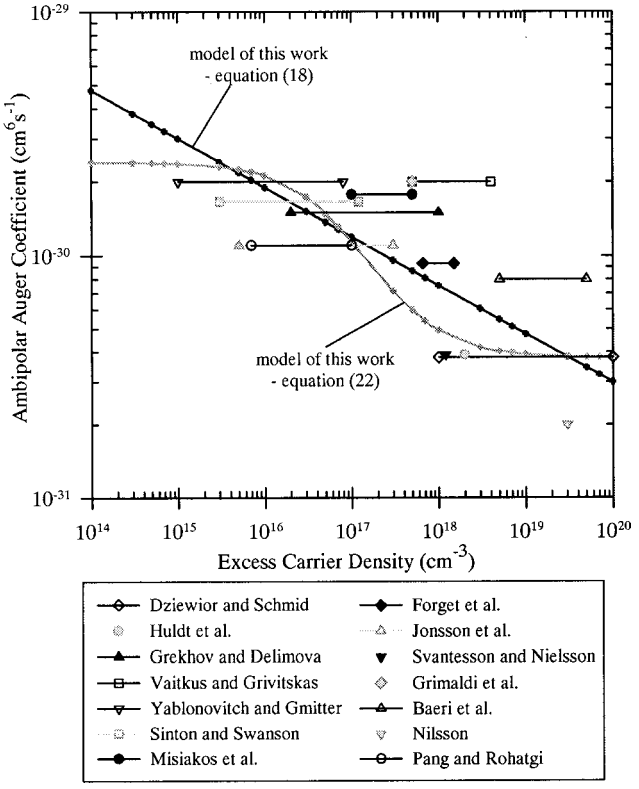

FIG. 6. Values for the ambipolar Auger coefficient as a function of excess carrier density from the models of this work, Eqs. (18) and (22). Equation (18) is based on simply fitting high injection lifetime data, while Eq. (22) is also constrained by the Mott density (see Sec. V for a discussion). Published values for the ambipolar Auger coefficient are included (see Refs. 6, 14, 20, 26–36).

time and therefore we conclude that the Auger model of Eq. (20) also works well with *p*-type silicon.

V. DISCUSSION

As shown in the previous section, the general parameterization determined for Auger recombination in silicon successfully fits the available lifetime data for arbitrarily doped and arbitrarily injected silicon. It is clear that Auger recombination is enhanced above the *ideal* inverse quadratic rate and a number of possible explanations for this have been given, the most convincing being Coulombic interactions between the charge carriers. Unfortunately, the scatter in the available data does not permit us to conclude that Coulomb enhancement is the single reason for the enhanced rate. Indeed, there are a number of possible parameterizations that could be used to fit the available lifetime data equally well, particularly for the low injection lifetime data. One could satisfactorily use the low injection lifetime parameterizations of Altermatt *et al.* [given in Eqs. (6) and (7) here] along with our parameterization for the injection level dependent ambipolar Auger coefficient [Eq. (18)] to obtain another valid description of Auger recombination.

If Coulomb enhancement is the dominant reason for the increased Auger recombination rate, then it is theoretically expected that once the majority carrier concentration or the injection level exceed the exitonic Mott density of approximately 1×10^{18} cm^{-3} at 300 K,[10] the formation of excitons will be greatly reduced due to screening effects. Therefore, the rate of Auger recombination should converge to the ideal rate (i.e., $\tau_A \propto 1/n^2$). The low injection Auger lifetime model of Altermatt *et al.* was formulated to meet this requirement. It is also possible to parameterize the injection level dependent ambipolar coefficient to fit the Auger lifetime data of Yablonovitch *et al.* and satisfy this Mott transition constraint. We would thus obtain

$$C_a^* = 3.79\times10^{-31}\left(\frac{\Delta n + 3.8\times10^{17}}{\Delta n + 6\times10^{16}}\right). \tag{22}$$

The coefficient at the front is just the sum of $C_n + C_p$ from Dziewor and Schmid. A comparison of the two parameterizations for C_a^* [Eqs. (18) and (22)] is given in Fig. 6. It can be seen that for excess carrier levels between 3×10^{15} cm^{-3} and 1×10^{17} cm^{-3} (the range measured by Yablonovitch *et al.*) they agree quite well. However, outside this range the two parameterizations are quite different. For lower excess carrier levels, the predicted Auger lifetimes are very high ($\geqslant$100 ms) and it is therefore not possible to probe this range to verify either parameterization, as lifetimes greater than 50 ms have never been measured in silicon. Included in Fig. 6 are the values for the ambipolar Auger coefficient determined by a number of authors for excess carrier densities greater than 1×10^{15} cm^{-3}. There is significant scatter in the reported values and both of our parameterizations for the ambipolar Auger coefficient fall within this scatter. Thus, the existing experimental data are not sufficiently accurate to verify one parameterization over the other and therefore determine if a transition at the exitonic Mott density occurs. A more accurate determination of the ambi-

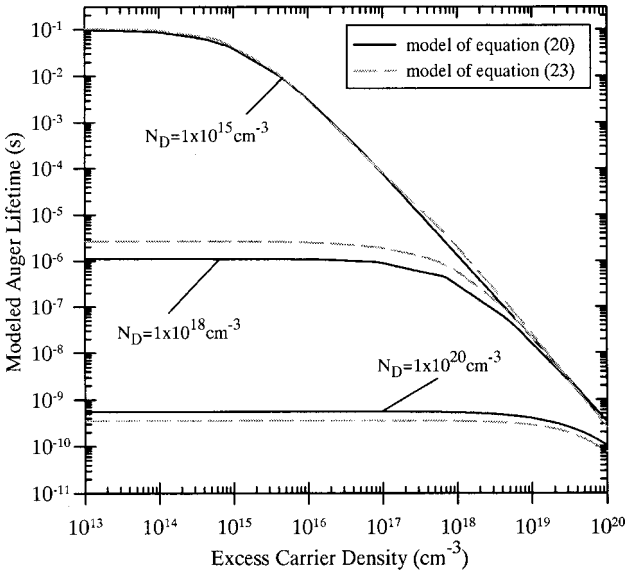

FIG. 7. Comparison of the Auger lifetime of *n*-type silicon with various doping densities predicted by the two models determined in this work. The model of Eq. (23) is constrained by the Mott transition.

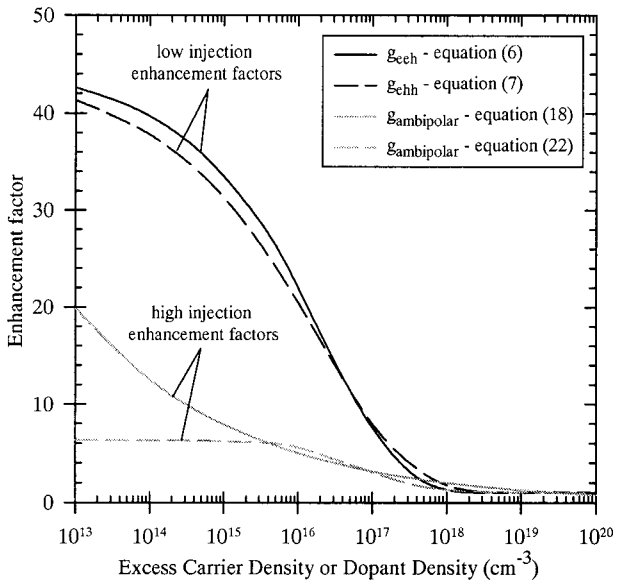

FIG. 8. Comparison of the enhancement factor of the Auger recombination rate for highly injected, lowly doped silicon compared to lowly injected, highly doped silicon. The enhancement factor is lower for highly injected silicon consistent with the Coulomb-enhanced Auger recombination theory of Hangleiter and Hacker (see Ref. 4).

polar Auger coefficient for excess carrier densities in the range of 1×10^{17} cm^{-3} to 1×10^{19} cm^{-3} is needed to clarify this issue.

A complete parameterization for the Auger recombination rate using the ambipolar Auger coefficient of Eq. (22), such that the Mott transition occurs [based on Eqs. (6), (7), (19), and (22)], would be

$$R_{\text{Auger}}=np\left[2.8\times10^{-31}n_0\left(1+44\left\{1-\tanh\left[\left(\frac{n_0}{2\times10^{16}}\right)^{0.29}\right]\right\}\right)+9.9\times10^{-32}p_0\left(1+44\left\{1-\tanh\left[\left(\frac{p_0}{2\times10^{16}}\right)^{0.29}\right]\right\}\right)+3.79\times10^{-31}\Delta n\left(\frac{\Delta n+3.8\times10^{17}}{\Delta n+6\times10^{16}}\right)\right]. \quad (23)$$

Note that we have adjusted some of the parameters in Eqs. (6) and (7) to be consistent with Ref. 15. This is necessary or some of the predicted lifetimes would be less than the measured lifetimes in Figs. 4 and 5.

Representative modeled Auger lifetimes for the parameterizations of Eqs. (20) and (23) are plotted in Fig. 7. The main deviations between the two models are expected to be in determining the low injection Auger lifetime for doping densities in the range of 1×10^{17} cm^{-3} to 5×10^{18} cm^{-3} as mentioned in Sec. III A, and to a lesser extent, for highly injected samples with excess carrier densities in the same range. This can indeed be seen in Fig. 7. In general, however, the two models are in relatively good agreement.

A comparison of the enhancement of the Auger recombination rate, above the ideal rate, for lowly injected, intermediately doped silicon versus lowly doped but highly injected silicon can be made using the parameterizations given earlier. Reasonable values for the enhancement factors for lowly injected silicon as a function of doping density, g_{eeh} and g_{ehh}, are given by Eqs. (6) and (7). Values for the enhancement factor for highly injected silicon as a function of injection level, $g_{\text{ambipolar}}$, are given by Eqs. (18) and (22) divided by the $C_n+C_p=3.79\times10^{-31}$ cm^6 s^{-1} value of Dziewior and Schmid. These four curves are plotted in Fig. 8. It is very clear that the enhancement factors for highly injected silicon are lower than for low injected, highly doped silicon. This is consistent with the theory of Coulomb enhancement by Hangleiter and Hacker. Further, it follows that modeling the Auger recombination rate with a single enhancement factor as attempted in Refs. 15 and 17 (see Sec. II C) is not possible.

It is important to stress that the parameterizations we have developed in this work fit the available experimental lifetime data. As such, they represent an upper limit on the Auger recombination rate or alternatively, a lower limit on the Auger lifetime. It is possible that with improved silicon growth technology and surface passivation techniques, higher lifetimes, and therefore lower rates of Auger recombination may be measured in the future.

Finally, throughout this work we have assumed that the rate of radiative recombination can be quantified using the constant $B=9.5\times10^{-15}$ cm^3 s^{-1}. In reality this is a simplification, as radiative recombination is also believed to be affected by Coulombic interactions.[23] The effect of this simplification is that any increase in the radiative recombination from the *ideal* rate given by Eq. (15), has actually been interpreted as Auger recombination. A more accurate determination of the doping and injection level dependence of radiative recombination would be required to more accurately assign the recombination events as either radiative or Auger. This may result in a small adjustment to our parameterization for Auger recombination. What can be concluded is that the

global rate of intrinsic recombination in silicon, $R_{\text{intrinsic}}$, can be expressed as

$$R_{\text{intrinsic}} = R_{\text{auger}} + R_{\text{rad}} = np(1.8\times10^{-24}n_0^{0.65} + 6 \times10^{-25}p_0^{0.65} + 3\times10^{-27}\Delta n^{0.8} + 9.5\times10^{-15}), \quad (24)$$

where the effect of the various enhancement process for both radiative and Auger recombination are quantified by the term in brackets. Indeed, the fact that intrinsic recombination is a composite of two particle and three particle recombination processes may explain the origin of the fractional exponents in the bracketed term of Eq. (24). The terms can be expected to have an exponent between 1 and 2 depending on the relative proportion of two particle (radiative) and three particle (Auger) recombination events.

VI. CONCLUSIONS

A parameterization for band-to-band Auger recombination in crystalline silicon at 300 K has been proposed and validated with lifetime measurements. This parameterization is a significant improvement over previous models, as it accurately fits the experimental lifetime data for arbitrary injection level and arbitrary dopant density, for both *n*-type and *p*-type dopants. We have confirmed that Auger recombination is enhanced above the traditional free-particle rate at both low injection and high injection conditions. Further, we have shown that the rate of enhancement is less for highly injected intrinsic silicon compared to lowly injected doped silicon, which is consistent with the theory of Coulomb-enhanced Auger recombination. Variations on the parameterization, such as requiring the rate of Auger recombination to converge to the traditional free-particle rate for carrier densities above the exitonic Mott density have been discussed.

ACKNOWLEDGMENTS

This work has been partly funded by the Australian Research Council. The authors wish to thank P. P. Altermatt for providing the data used in Figs. 1 and 2.

[1] R. F. Pierret, *Advanced Semiconductor Fundamentals* (Addison-Wesley, Reading, MA, 1989), Vol. VI.
[2] M. A. Green, *Silicon Solar Cells: Advanced Principles and Practice* (UNSW, Sydney, 1995).
[3] D. J. Roulston, *Bipolar Semiconductor Devices* (McGraw-Hill, New York, 1990).
[4] A. Hangleiter and R. Hacker, Phys. Rev. Lett. **65**, 215 (1990).
[5] M. S. Tyagi and R. Van Overstraeten, Solid-State Electron. **26**, 577 (1983).
[6] J. Dziewior and W. Schmid, Appl. Phys. Lett. **31**, 346 (1977).
[7] D. B. Laks, G. F. Neumark, and S. T. Pantelides, Phys. Rev. B **42**, 5176 (1990).
[8] A. Haug, Solid-State Electron. **21**, 1281 (1978).
[9] P. T. Landsberg, Appl. Phys. Lett. **50**, 745 (1987).
[10] P. P. Altermatt, J. Schmidt, G. Heiser, and A. G. Aberle, J. Appl. Phys. **82**, 4938 (1997).
[11] J. del Alamo, S. Swirhun, and R. M. Swanson, Proc. International Electron Devices Meeting Technical Digest, Washington, 1985, pp. 290–293.
[12] S. E. Swirhun, Y. H. Kwark, and R. M. Swanson, Proc. International Electron Devices Meeting Technical Digest, Washington, 1986, pp. 24–27.
[13] S. E. Swirhun, Ph.D. thesis, Stanford, 1987.
[14] P. Jonsson, H. Bleichner, M. Isberg, and E. Nordlander, J. Appl. Phys. **81**, 2256 (1997).
[15] P. P. Altermatt, J. Schmidt, M. J. Kerr, G. Heiser, and A. G. Aberle, Proc. 16th European Photovoltaic Solar Energy Conference, Glasgow, Scotland, 2000.
[16] P. P. Altermatt, R. A. Sinton, and G. Heiser, Sol. Energy Mater. Sol. Cells **65**, 149 (2001).
[17] J. Schmidt, M. J. Kerr, and P. P. Altermatt, J. Appl. Phys. **88**, 1494 (2000).
[18] D. A. Clugston and P. A. Basore, Proc. 26th IEEE Photovoltaic Specialists Conference, Anaheim, CA, 1997.
[19] S. W. Glunz, D. Biro, S. Rein, and W. Warta, J. Appl. Phys. **86**, 683 (1999).
[20] E. Yablonovitch and T. Gmitter, Appl. Phys. Lett. **49**, 587 (1986).
[21] T. F. Ciszek and T. H. Wang, Proc. 14th European Photovoltaic Solar Energy Conference, Barcelona, 1997, pp. 396–399.
[22] M. J. Kerr and A. Cuevas, Semicond. Sci. Technol. **17**, 35 (2002).
[23] H. Schlangenotto, H. Maeder, and W. Gerlach, Phys. Status Solidi A **21**, 357 (1974).
[24] M. J. Kerr, J. Schmidt, and A. Cuevas, Proc. 16th European Photovoltaic Solar Energy Conference, Glasgow, Scotland, 2000.
[25] A. G. Aberle, S. W. Glunz, and W. Warta, J. Appl. Phys. **71**, 4422 (1992).
[26] L. Huldt, N. G. Nilsson, and K. G. Svantesson, Appl. Phys. Lett. **35**, 776 (1979).
[27] I. V. Grekhov and L. A. Delimova, Sov. Phys. Semicond. **14**, 529 (1980).
[28] Y. Vaitkus and V. Grivitskas, Sov. Phys. Semicond. **15**, 1102 (1981).
[29] R. A. Sinton and R. M. Swanson, IEEE Trans. Electron Devices **ED–34**, 1380 (1987).
[30] K. Misiakos, J.-S. Park, and A. Neugroschel, J. Appl. Phys. **67**, 2576 (1990).
[31] B. C. Forget, D. Fournier, and V. E. Gusev, Appl. Phys. Lett. **61**, 2341 (1992).
[32] S. G. Svantesson and N. G. Nilsson, J. Phys. C **12**, 5111 (1979).
[33] M. G. Grimaldi, P. Baeri, and E. Rimini, Appl. Phys. A: Solids Surf. **A33**, 107 (1984).
[34] P. Baeri, M. A. Harith, G. Russo, E. Rimini, A. Giuletti, and M. Vaselli, Phys. Status Solidi B **130**, 225 (1985).
[35] N. G. Nilsson, Phys. Scr. **8**, 165 (1973).
[36] S. K. Pang and A. Rohatgi, Appl. Phys. Lett. **59**, 195 (1991).